Effect of Infill Parameters on Tensile Mechanical Behavior in Desktop 3D Printing

Article *in* 3D Printing and Additive Manufacturing · September 2016

DOI: 10.1089/3dp.2015.0036

4 authors:

Miguel Fernandez-vicente
Polytechnic University of Valencia
15 PUBLICATIONS **629** CITATIONS
SEE PROFILE

Wilson Calle
Politecnica Salesiana University
3 PUBLICATIONS **524** CITATIONS
SEE PROFILE

S. Ferrándiz
Polytechnic University of Valencia
93 PUBLICATIONS **1,609** CITATIONS
SEE PROFILE

Andres Conejero
Polytechnic University of Valencia
21 PUBLICATIONS **629** CITATIONS
SEE PROFILE

Preprint version. Final publication in 3D PRINTING AND ADDITIVE MANUFACTURING Volume 3, Number 3, 2016. It is available from Mary Ann Liebert, Inc., publishers http://dx.doi.org/10.1089/3dp.2015.0036

Effect of Infill Parameters on Tensile Mechanical Behavior in Desktop 3D Printing

Miguel Fernandez-Vicente,[1] Wilson Calle,[2] Santiago Ferrandiz,[3] Andres Conejero[1]

Abstract

The recent creation and growth of desktop 3D printing has led to a new way of building objects. In the manufacture of pieces using Open Source 3D printing it is very common to use a range of infill patterns and densities with the aim of reducing printing time and material consumption. However, it is not well understood how these factors influence the characteristics of the pieces obtained. Due to the differences with FDM technology, it is necessary to evaluate the strength of the pieces manufactured with this technology. In this work, has been evaluated the influence of two controllable variables: pattern and density of the infill. A series of test pieces with different density characteristics and infill patterns was produced using an open source 3D printer. The results obtained show that the influence of the different printing patterns causes a variation of less than 5% in maximum tensile strength, although the behaviour is similar. The change in infill density determines mainly the tensile strength. The combination of a rectilinear pattern in a 100% infill shows the higher tensile strength, with a value of 36.4 Mpa, with a difference of less than 1% from raw ABS material.

Keywords: 3D printing, fused filament fabrication, FDM, infill pattern, mechanical strength, mesostructure

Introduction

Additive Manufacturing (AM), also called rapid prototyping, since its origins in the 80s has been a useful tool for the process of design and development of products, and often represents considerable saving in time in this process.[1] For the addition of material, there are different AM techniques, based mainly on 3 types of construction: solidification of a liquid, sintering or fusion of powder, and deposition of material. With each of these techniques, several different systems have been patented, such as Stereolithography (SLA), Selective Laser Sintering (SLS), or Fused Deposition Modelling (FDM).[2]

The expiration of those patents, first of FDM technology, and later SLA and SLS, is leading to a growth in interest in developing and improving these technologies. The seed of this interest is the RepRap project, which aims to create a self-replicating manufacturing machine. A three-dimensional (3D) printing machine that uses a manufacturing technique similar to FDM technology was designed, but to avoid legal problems it was named FFF technology (Fused Filament Fabrication).[3] One characteristic of this new approach was to build the machines small enough to be desktop 3D printers, opening the door to a new industry currently called "desktop 3D printing". The disruptive yet successful elements of this approach were to share on the internet the design and building instructions for the construction of a similar machine by any one and the inclusion in the design of a large percentage of the pieces built by the same machine. This means that a single machine can fabricate pieces for the building of other machines, creating an exponential growth in the number of users, new designs, and developments that have never been done by the patent owner.[4] A great number of desktop 3D printing companies have emerged from this project and have experimented a significant growth in the number of sold systems. The average estimated growth of unit sales over the past four years (2011-2014) was of a 135.2%. The estimation of desktop 3D printers sold is of 72500 in 2013 to near 140000 in 2014.[5]

Literature review

The process of 3D printing with FFF technology consists of pushing a thermoplastic filament using an extruder element into a fusion chamber, known as a *hotend*. The fused material is pushed through the tip of the hotend, and it is deposited in a controlled way, normally at an inferior distance than the diameter of the tip hole. The process from the digital design to the deposition needs to transform the 3D geometry into movement

[1] Instituto de Diseño y Fabricación, Universitat Politècnica de València, Valencia, Spain.
[2] Departamento de Ingeniería Mecánica Automotriz, Universidad Politécnica Salesiana del Ecuador, Cuenca, Ecuador.
[3] Departamento de Ingeniería Mecánica y Materiales, Universitat Politècnica de València, Valencia, Spain.

commands, known as G-code. These commands are interpreted by the machine control electronics, which deposits the material where it is needed.

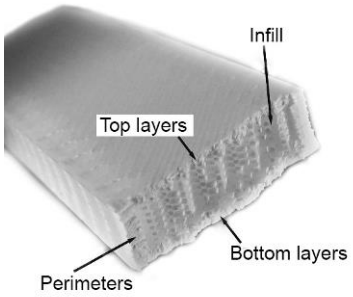

FIG. 1. Section of the printed specimens. Characteristic areas.

In the structure of FDM or FFF parts four characteristic zones can be distinguished that can be seen in FIG. 1. The first deposited zone comprises several solid layers that form the lower area of the outside of the piece. Next the main body of the piece is built, in which a set of perimeter filaments are deposited. The interior is built using an infill of a density and mesostructure that can be controlled. In FDM the term "air gap" refers to the space between deposited filaments in this zone.[6] Although in FFF it can be controlled the infill percentage, the air gap value cannot be specified, and consequently the real density value varies among printers and software stacks.[7] In the structure of printed parts finally the top layers are deposited, which are usually solid, to close the exterior of the piece.

Process characterization

The internal structure of a FDM part is not significantly different from that of a fibre reinforced composite, as it can be interpreted as a composite structure with vertically stacked layers of polymer fibers, and air.[8,9] In FDM, a solid filament is extruded in a semi-molten state and solidified in chamber at a temperature below Tg of the material. The temperature changes from Tm to Tg in around 0.55 s.[10] As a consequence, volumetric shrinkage takes place, developing weak fiber bonding, and high porosity of the structure.[11]

The bond quality between filaments depends on envelope temperature and variations in the convective conditions,[12] as a molecular diffusion and cross-linking between the polymer deposition is needed.[11] As the deposition of material generally is done by a single head, the deposition pattern has a significant effect on the part stresses and deflections.[13] The accumulation of residual stresses can bring about warp, inner-layer delaminating or cracking.[14,15]

There are many variables that may have an effect on the characteristics of the object manufactured.[16] These characteristics have been studied mainly by three aspects: surface quality, dimensional accuracy, and mechanical behaviour. On surface quality Boschetto *et al.* (2013) developed a mathematical model of the surface profile, in order to determine the best object orientation.[17] The mechanical and dimensional characteristics have been objective of studies since the early years of FDM technology. By 1996 Fodran *et al.* studied the tensile behaviour and dimensional integrity with different flow rates and bonding agents.[18]

One of the characteristics that has received a great deal of attention in the literature is mechanical behaviour. Rodriguez *et al.* developed a series of studies in order to study the mechanical behaviour of acrylonitrile butadiene styrene (ABS) fused deposition. First, they characterized the mesostructure of the materials.[10] Second, they studied the tensile strength of single raw filament and tested unidirectional FDM specimens. Additionally, they measured the polymer chain orientation,[19] as the raster orientation causes alignment of polymer molecules along the direction of deposition.[11] Finally, they developed an analytical model for unidirectional FDM ABS, using laminate theory, and concluded that the form of the voids shows a remarkable influence in mechanical properties. Furthermore, they observed that the change in the infill angle changes the fracture from ductile to brittle. This is due to the dependence on the bonding between filaments.[20,21]

The complexity of such structure determines an anisotropic behaviour. The variables that influence this characteristic can be classified in: material properties, build specifications, part positioning and orientation, and environment.[22] Ahn *et al.* (2002) studied this anisotropic behaviour taking into account variables from the different classifications, analysing the tensile and compressive strength. In this study it was concluded that air gap and raster orientation have more influence than other variables.[6] A similar study was developed by Ziemian *et al.* (2012). They evaluated the raster orientation effect in the direction of the strain. Tests for tensile, compression, flexural, impact and fatigue were developed, and the results were then compared with the properties of injected sample pieces. From this study the optimal factor levels to improve strength were obtained.[23]

Some studies have developed models for prediction of mechanical behaviour. Bellini and Güçeri (2003) presented a methodology to determine the stiffness matrix, interpreting the structure as orthotropic, and compared the results with experimental tests.[8] Croccolo *et al* (2013) studied the effect of the number of contours in tensile strength. They developed an analytical model to predict the mechanical behaviour and verified it with experimental results. The model is consistent in the elastic field, but unable to predict

Preprint version. Final publication in 3D PRINTING AND ADDITIVE MANUFACTURING Volume 3, Number 3, 2016. It is available from Mary Ann Liebert, Inc., publishers http://dx.doi.org/10.1089/3dp.2015.0036

the nonlinear behaviour of the material.[24] Gurrala and Regalla (2014) developed a mathematical model for tensile strength by prediction of bonding surface between fibers. Their results show that the temperature is not enough to fully cross-link the fibers.[21]

Regarding the study of different infill structures, Baich and Manogharan (2015) analysed the correlation between cost and time based on infill pattern and desired mechanical properties using a production-grade FDM system. They concluded that solid infill has greater strength performance than double-dense infill at the same production cost. This study also highlights the need of additional analysis of "custom" infill patterns with respect to mechanical loading.[25]

Mechanical behaviour in FFF technology

Although FFF technology is similar to FDM, there are a series of factors that open new areas to study. However, due to the novel development of FFF technology, there are few studies on this technology.

One of those factors is the uncontrolled environment parameters, as Tymrak *et al.* (2014) based their study. Furthermore, in their study were used different machines with different slicing and control software, as well as different extrusion temperatures and materials. In their study the specimens were printed with 100% infill, but the uncontrolled air gap derived in a wide dispersion of results. Higher mechanical properties than similar studies on FDM were obtained, although the raw filament mechanical characteristics were not determined.[7]

Lanzotti *et al.* (2015) studied the influence of layer thickness, infill orientations, and the number of shell perimeters, but obtained only the polylactic acid (PLA) mechanical characteristics.[26] Rankouhi *et al.* (2016) analysed the same parameters using ABS, layer thickness and orientation, and performed a fractography to determine the failure modes. They observed that smaller layer thickness increases the strength and that large Air Gap causes interlayer fusion bonds to fail.[16]

Akande *et al.* (2015) studied the significance of layer thickness, fill density, and speed of deposition on the mechanical properties. Furthermore, they developed a low-cost test jig and compared it with conventional testing machine, obtaining a valid method for quality testing.[27] Qureshi *et al.* (2015) synthetized the parameters analysed in previous studies, and selected a list of 13 controllable factors which may affect the mechanical behaviour. The mean ultimate tensile strength (UTS) obtained was similar to earlier research. They used a Taguchi's method of design of experiment to obtain the optimised parameters values.[28]

Lanzotti *et al.* (2015) made an analysis of the effects on the dimensional accuracy when changing three of the deposition variables (layer thickness, deposition speed, and flow rate), and found a recommended combination of these.[29] Afrose *et al.* (2015) studied the static strength and fatigue behaviour of PLA material with different orientations. They obtained a 60% tensile stress of that of injection moulded PLA material.[30]

Nonetheless, until now there has been no study that evaluates the different patterns that can be selected in the infill, or the influence of their density on mechanical strength. These parameters can be controlled in this Open Source technology, but couldn't be controlled in FDM technology. For this reason, the aim of this study is to evaluate the influence in this technology of two parameters, the pattern and the density of the infill, emulating the printing conditions of an inexpert user. With these two objectives in mind, the mechanical characteristics of the raw material were obtained, and were compared with the three most common pattern types, and three infill densities.

TABLE 1. Values of the Most Characteristics Fixed Parameters

Parameters	*Value*	*Units*
Bed temperature	110	ºC
Nozzle temperature	230	ºC
Layer thickness	0.3	mm
Perimeters	3	
Solid top layers	3	
Solid bottom layers	3	
Infill pattern top/bottom	Rectilinear	
Infill angle	45	ºC
Extrusion width first layer	200	%

Materials and methods

A series of specimens were produced using an open source desktop 3D printing machine in order to emulate the fabrication conditions of an inexpert user of this type of technology. Due to the existence of a very large range of options of mechanical and electronic configurations, and software chains, listed below are the more relevant details of the configuration of the equipment used for this study.

The structure of the 3D printer was the model RepRap Prusa i3, one of the more widespread models nowadays.[31] The tip for the fabrication had a diameter of 0.5 mm. The control electronics of the machine was the Arduino Mega board, the RAMPS v1.4 adaptation board, and motor drivers A4988. The firmware loaded in the board was Marlin version 1.0.

Preprint version. Final publication in 3D PRINTING AND ADDITIVE MANUFACTURING Volume 3, Number 3, 2016. It is available from Mary Ann Liebert, Inc., publishers http://dx.doi.org/10.1089/3dp.2015.0036

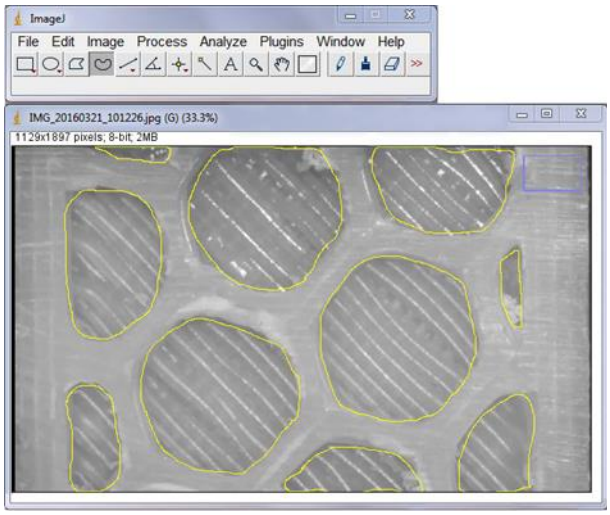

FIG. 2. Density analysis on ImageJ software.

Regarding the software and printing configurations, the toolpath calculation was made with the open source software Slic3r version 1.0.[32] With this software, a range of parameters can be controlled, and modifications to these could lead to the improvement in the results. However, a particular set of parameters could not be transferred to other geometries. Moreover, one of the objectives of the study would be lost: to emulate the printing conditions of an inexpert user. Therefore, the predefined configurations of the software were used. The values of the most characteristic parameters are listed in TABLE 1. The specimens were printed without raft, a previous grid to improve adherence, as bed heating and adhesion were good enough to avoid it.

In this study, the infill of the intermediate zone was modified. The parameters evaluated in this study were the infill density and pattern. For the infill, three levels were evaluated: 20%, 50%, and 100%. The first level is the predefined by the software; the last one was selected to obtain information about the behaviour with full infill; the intermediate level, 50%, was chosen to evaluate how the evolution of mechanical behaviour between the other two levels is. For the infill pattern, due to the capabilities of the software, it is possible to use eight types of patterns. However, only the three most widely used were selected: line, rectilinear, and honeycomb. Line pattern generates a random infill pattern with linear connections between the walls. Rectilinear pattern creates a rectangular mesh, predefined at 45º from the machine axis. Honeycomb pattern produces a structure of hexagonal cells similar to a honeycomb.[33] A measurement of the printed density was carried out with the aim of detect possible causes of mechanical behaviour. The methodology used for measurements was image analysis. The images were captured with the aid of an Olympus CH2 microscope (Olympus Optical Co., Ltd., Tokyo, Japan), and were analysed using ImageJ software (National Institutes of Health, Bethesda, Maryland), as can be seen on Figure 2. The values measured presented an average deviation of less than 6% from the virtual density.

For the evaluation of the dispersion, and according to the standard, five test pieces were produced with each combination of printing parameters considered as variables. FIG. 3a-f shows screenshots of the different patterns: (a) Rectilinear, (b) Honeycomb, (c) Line, and a representation of the infill density with the rectilinear pattern with values of (d) 20%, (e) 50% (f) 100%.

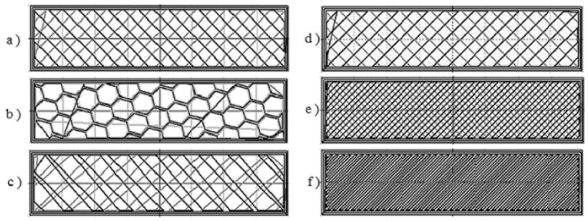

FIG. 3. Infill patterns (a) rectilinear, (b) honeycomb, (c) line, and densities (d) 20%, (e) 50%, and (f) 100% used as variables.

The material used for the manufacturing of the test pieces was 3-mm diameter filament of ABS (ABS Nature, Torwell Technologies Co. Shenzhen, China). Although the manufacturer provides information of the material [34], to obtain the reference values for the behaviour and strength of the material, injection-moulded sample pieces were tested. The same ABS filaments used for printing the test pieces were cut into pellets in a plastic shredder, and another series of injection-moulded test pieces were tested in accordance with ISO 527. The values obtained from the test were: An ultimate strength of 36.56 MPa and an elasticity modulus of 1826 MPa.

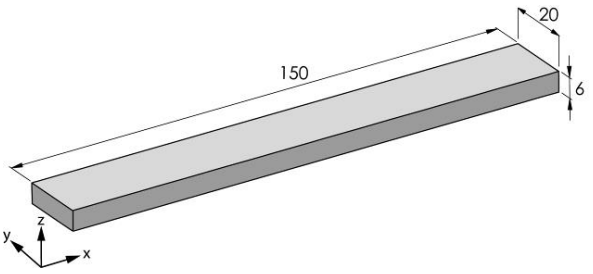

FIG. 4. Test specimen dimensions in mm and print orientation.

The same standard was used as a reference for the tensile test and the design of the pieces. However, in order to avoid the stress concentration at transition zones of specimens head, as tested by Croccolo *et al.* (2013),[24] and to leave enough space for the infill geometry, the pieces were designed without a bigger clamp connection, as can be seen in FIG. 4. Some previous studies, to avoid the same problem,

Preprint version. Final publication in 3D PRINTING AND ADDITIVE MANUFACTURING Volume 3, Number 3, 2016. It is available from Mary Ann Liebert, Inc., publishers http://dx.doi.org/10.1089/3dp.2015.0036

TABLE 2. Average tensile characteristics of the different mesostructures for ABS FFF 3D printed specimens

Infill pattern	*Infill density*	*Tensile strength (MPa)*	*Tensile strain (%)*	*Elastic modulus (MPa)*	*Weight (g)*
Line	20	16.00	4.76	499	11.06
Line	50	20.06	4.86	640	13.98
Line	100	35.68	5.30	784	17.54
Rectilinear	20	15.62	5.30	408	10.64
Rectilinear	50	19.58	4.62	659	13.98
Rectilinear	100	36.40	5.36	834	19
Honeycomb	20	16.52	4.44	568	11.22
Honeycomb	50	21.78	4.38	745	14.76
Honeycomb	100	36.10	5.42	802	18.88
Raw ABS	-	36.56	5.44	1826	

tested an adapted specimen geometry from the standard ASTM D3039.[6,16,19] In this study, a preliminary experiment was carried out in order to analyse the suitability of this geometry, and the results were admissible.

All specimens were fabricated in the horizontal plane, where the orientation of the fibres and their bonding is better than in other planes.[23] One factor that determined this situation was the infill pattern, as until now, it cannot be oriented in different planes, and remains in the X-Y plane. Only one orientation of specimens was used, along X-axis as shown in Figure 4, in order to obtain results dependent upon the fiber-to-fiber fusion, and consecuently the internal mesostructure.[23] Therefore, the specimens were formed with a total of 20 layers.

The tensile strength tests were performed in an Instron model 5967 double column universal test machine, with a load capacity of 30 kN. Before the tests were done, a software calibration of the load cell was performed. The tests were carried out according to the ISO 527, with a preload of 20 N, and a test speed of 2 mm/min.

Results and discussion

The results obtained from the test show differences between the different pairs of parameters of infill density and pattern, also called mesostructures, of the specimens.

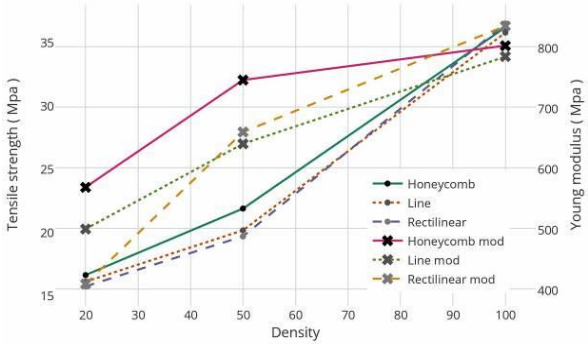

FIG. 5. Tensile strength and Young's modulus evolution with density change.

As can be seen in TABLE 2, a higher level of density resulted in a lower amount of voids in the infill, and subsequently, higher tensile strength. This situation is similar for the three types of infill patterns, especially in the rectilinear pattern, where at 20% density, the tensile strength is the lowest, but at 100%, the value is the highest of all of the results, 36.4 Mpa. An additional column with average specimen weight has been added to evaluate its influence.

Observing the change in the stiffness in the specimens, with the elastic modulus, this value increases as the density increases. To evaluate these changes, FIG. 5 shows the comparison between the change in the tensile strength, whose values are from the left y-axis, and the change in the Young's modulus, using the right y-axis as reference for the values.

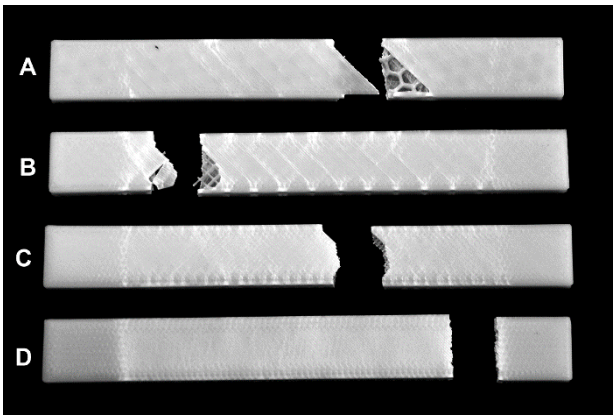

FIG. 6. Examples of tested specimens. A: Honeycomb 20%. B: Rectilinear 20%. C: Rectilinear 50%. D: Rectilinear 100%.

An increase in the tensile strength of the three patterns can be observed, with a very similar evolution in the values. From 20% to 50% the value increases, but the change is more significant between 50% and 100%. This situation is different in the case of the elastic modulus, as from 20% to 50% there is an increase, but it is smaller than that from 50% to 100%.

This difference may be due to the ability of the infill fibres to deform and absorb the stress prior

Preprint version. Final publication in 3D PRINTING AND ADDITIVE MANUFACTURING Volume 3, Number 3, 2016. It is available from Mary Ann Liebert, Inc., publishers http://dx.doi.org/10.1089/3dp.2015.0036

to a break in the bonds between the different fibres. This capability increases as the density also increases. When that density starts to create bonds between the different sections of the pattern, the tensile strength improves. However, the increase in the ability to deform is reduced.

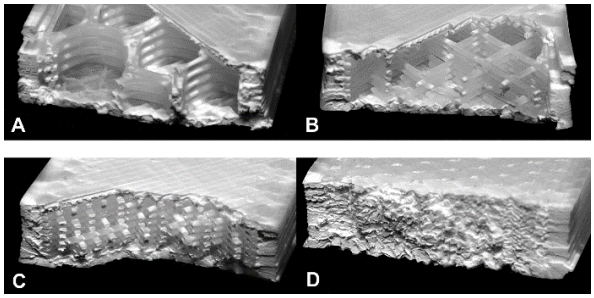

FIG. 7. Fracture detail of example tested specimens.

In FIG. 6 and FIG. 7 four representative examples of tested specimens can be seen to illustrate the failure mode. The fracture in other specimens with different parameters is similar. The sample specimens A and B show two different infill patterns with the lowest density. In FIG. 6 the different stress distributions are visible in each of the infill densities. It is especially visible comparing B, C and D specimens, where the distance between the whitening areas reveals the pattern size.

Looking closely into the fracture zones in FIG. 7, a failure that occurred across the layers can be observed, in intralayer and interlayer bonds. A decrease in the interlayer bond failure can be seen from specimens C and D, although it is still present. These results are in agreement with those obtained by previous studies.[16,21] Comparing specimens A and B, it can be observed how the failure follows the weaker zones in the pattern, where there is less material. The upper layer failed along the 45º line. This reveals repeated failures of individual filaments by shearing and tension as observed in earlier studies. [6,35]

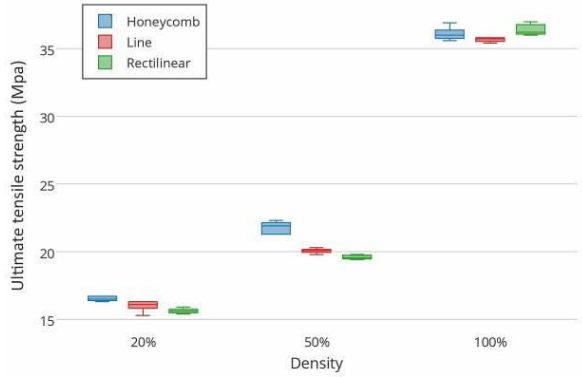

FIG. 8. Tensile strength box plot.

Interestingly, it can be seen that the bonding zones between different layers is different on each pattern. In the honeycomb pattern, each layer lays down on a similar previous layer. In the rectilinear pattern, the bonding zone between each layer corresponds only with the points where the filament crosses the previous layer filaments. This characteristic can be a possible explanation of why the honeycomb pattern shows higher elastic modulus. However, the variation of weight and stress distribution between patterns could be the reasons too. These results therefore need to be interpreted with caution.

To evaluate the deviation of the tests, next figures show the results in a box plot. FIG. 8 shows the results in the tensile strength grouped according to infill density, and FIG. 9 shows the Young's modulus with the same configuration as the previous figure.

Less than 2 Mpa difference can be observed between each pattern generally. The Honeycomb pattern generally shows the higher values of the three patterns. However, this can be due to a higher density, as can be observed in TABLE 2. An exception is in the 100% infill density, were the Rectilinear pattern is higher. This may be due to an inability of the software to generate a full infill with the other two patterns. These relationships may partly be explained by the slightly variation of weight, and consequently the density, between patterns of the same virtual density as can be seen in Table 2.

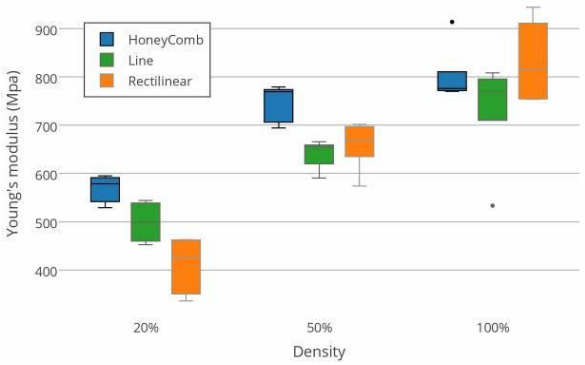

FIG. 9. Elastic modulus box plot.

On the other hand, in FIG. 9 the dispersion of the measures of the Young's modulus is higher than in the tensile strength evaluation. The comparison between the different patterns shows an improvement in the dispersion for the 50% infill density. Although the stiffness increases between 20% and 50%, the dispersion of the values is higher as the density increases. The reason may be explained due to the lack of control in the environment temperature. As discussed before, the bonding between the different fibres is crucial to the mechanical characteristics in this process. Therefore, the thermal conditions of the environment clearly affect the bonding conditions of the different samples [36].

Taking into consideration the dispersion of the data in FIG. 9, it is necessary to evaluate the evolution and dispersion of the stress during the test. FIG. 10 shows a graph of the strain-stress

Preprint version. Final publication in 3D PRINTING AND ADDITIVE MANUFACTURING Volume 3, Number 3, 2016. It is available from Mary Ann Liebert, Inc., publishers http://dx.doi.org/10.1089/3dp.2015.0036

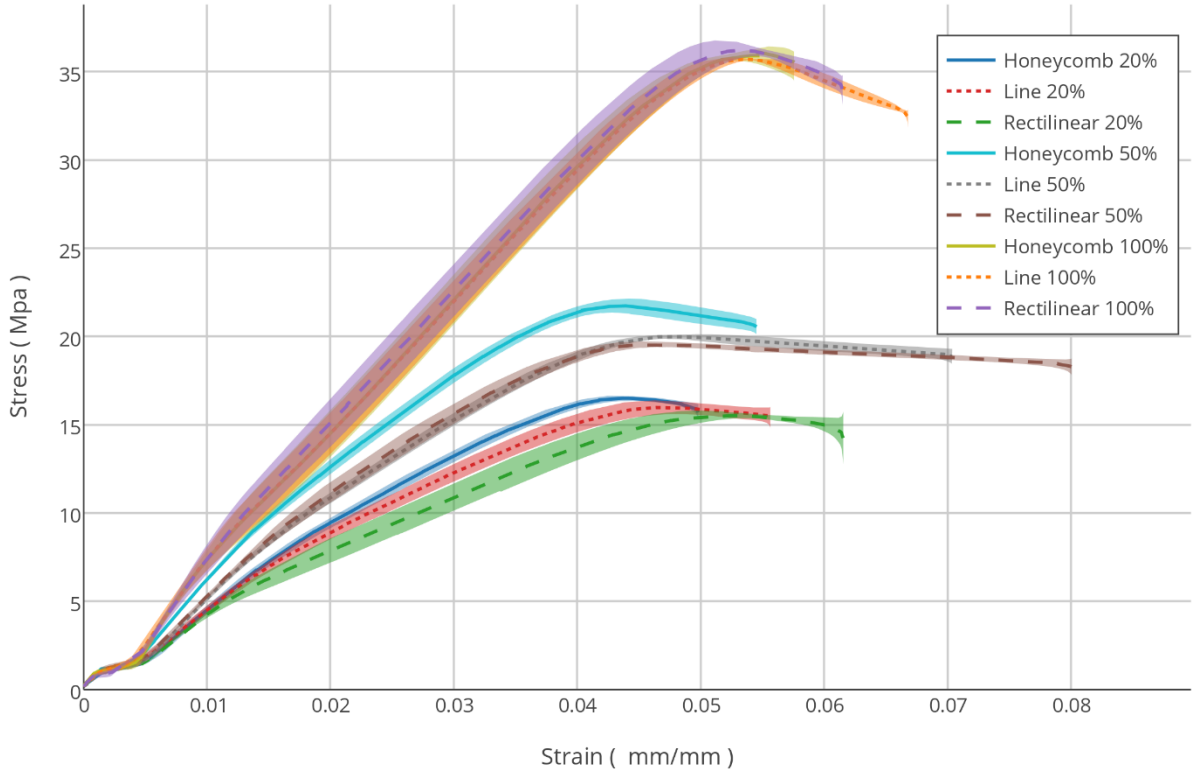

FIG. 10. Strain-stress diagram of the different mesostructures.

relation. In addition to the usual representation of the average value of the different mesostructures, the standard deviation of the different samples in each step of the data capturing is also shown. This deviation is expressed as a shadow in the same colour as the average value of the mesostructure. The upper limit of the shadow is the average value plus the standard deviation, and the lower limit corresponds to the average value minus the standard deviation.

As seen in FIG. 10 , the behaviour of the different mesostructures corresponds to the normal behaviour of the raw ABS material, with a similar elastoplastic transition, and a ductile break. In general, the deviations in the measurements are smaller than 5% of the value, with the exception of the rectilinear in 100% of infill, which is between 5% and 10% of deviation.

TABLE 3. Analysis of Variance with Lack-of-Fit of the squared-x model

Source	*Sum of Squares*	*df*	*Mean Square*	*F-ratio*	*p*
Model	3315.34	1	3315.34	6898.89	0
Residual	20.6642	43	0.480562		
Lack-of-Fit	0.021498	1	0.021498	0.04	0.8353
Pure Error	20.6427	42	0.491492		
Total(Corr.)	3336.01	44			

A stiffer behaviour of the honeycomb than the other two patterns was observed, resulting in better tensile strength. As commented before, this situation changes in the 100% infill density possibly due to the software algorithm.

A squared-x model to describe the relationship between the tensile strength with the density modification was as follows:

$$\sigma_p = 15.2364 + 0.002083 \cdot x^2, \quad (1)$$

where σ_p is the predicted tensile strength and x is the infill density.

This model was evaluated with a lack-of-fit test. An ANOVA analysis was then carried out, as can be seen in TABLE 3.

The test was performed by comparing the variability of the current model residuals to the variability between observations at replicate values of the independent variable X. Since the *p*-value for lack-of-fit in the ANOVA table is greater or equal to 0.05, the model appears to be adequate for the observed data at the 95.0% confidence level.

Conclusions

In this research, the significant effects of infill density and pattern on mechanical properties of the desktop FFF 3D printing process have been experimentally studied. Practical findings in the 3D printing process showed that:

- The combination of rectilinear pattern in a 100% infill shows the highest tensile strength, with a value of 36.4 Mpa, a difference of less than 1% from that of raw ABS material.
- Under the same density, the honeycomb pattern shows a better tensile strength,

Preprint version. Final publication in 3D PRINTING AND ADDITIVE MANUFACTURING Volume 3, Number 3, 2016. It is available from Mary Ann Liebert, Inc., publishers http://dx.doi.org/10.1089/3dp.2015.0036

although the difference between the different patterns is less than 5%. This discrepancy could be attributed to small variations of amount of plastic deposited for each pattern.

- The deposition trajectories and consequently the interlayer bonding zones is very different between honeycomb and rectilinear patterns. This could be a reason to explain the elastic modulus difference. However, more research on this topic needs to be undertaken before this association could be more clearly understood.
- The change in the infill density determines mainly the tensile strength, and the stiffness, especially between 20% and 50%.
- The mechanical behaviour between the different mesostructures is similar, and the dispersion between the samples is below 10%.
- The relationship between infill density and tensile strength can be fitted in a squared-X model.

Further studies are needed to understand the crystallinity volume fraction of the samples as previous studies developed on PLA, as it was observed a strong relationship between this characteristic and the tensile strength.[37]

The scarcity of studies in literature about the influence of mesostructure, as well as other factors such as environment, reveal a need for further research into the mechanical behaviour of the 3D printed pieces.

Acknowledgments

The authors wish to acknowledge the support of Prof. Juan A. García-Manrique and the composites manufacturing research group from UPV for providing the equipment to perform the tensile test.

Author disclosure statement

No competing financial interests exist.

References

1. Chua CK, Leong KF. Rapid Prototyping: Principles and Applications. Vol 1. World Scientific; 2003.
2. Gibson I, Rosen DW, Stucker B. Additive Manufacturing Technologies. Springer-Verlag New York; 2010.
3. Jones R, Haufe P, Sells E, et al. RepRap – the replicating rapid prototyper. Robotica. 2011;29(1):177-191.
4. de Bruijn E. On the viability of the open source development model for the design of physical objects. Lessons learned from the RepRap project. 2010.
5. Wohlers T. Wohlers Report 2015.; 2015.
6. Ahn, Montero, Odell, Roundy, Wright. Anisotropic material properties of fused deposition modeling ABS. Rapid Prototyp J. 2002;8(4):248-257.
7. Tymrak BM, Kreiger M, Pearce JM. Mechanical properties of components fabricated with open-source 3-D printers under realistic environmental conditions. Mater Des. 2014;58:242-246.
8. Bellini A, Güçeri S. Mechanical characterization of parts fabricated using fused deposition modelingn. Rapid Prototyp J. 2003;9(4):252-264.
9. Sood AK, Ohdar RK, Mahapatra SS. Parametric appraisal of mechanical property of fused deposition modelling processed parts. Mater Des. 2010;31(1):287-295.
10. Rodriguez JF, Thomas JP, Renaud JE. Characterization of the mesostructure of fused-deposition acrylonitrile-butadiene-styrene materials. Rapid Prototyp J. 2000;6(3):175-186.
11. Es-Said O, Foyos J, Noorani R, Mendelson M, Marloth R, Pregger BA. Effect of Layer Orientation on Mechanical Properties of Rapid Prototyped Samples. Mater Manuf Process. 2000;15(1):107-122.
12. Sun Q, Rizvi GM, Bellehumeur CT, Gu P. Effect of processing conditions on the bonding quality of FDM polymer filaments. Rapid Prototyp J. 2008;14(2):72-80.
13. Nickel AH, Barnett DM, Prinz FB. Thermal stresses and deposition patterns in layered manufacturing. Mater Sci Eng A. 2001;317(1–2):59-64.
14. Wang T-M, Xi J-T, Jin Y. A model research for prototype warp deformation in the FDM process. Int J Adv Manuf Technol. 2007;33(11-12):1087-1096.
15. Zhang Y, Chou K. A parametric study of part distortions in fused deposition modelling using three-dimensional finite element analysis. Proc Inst Mech Eng Part B J Eng Manuf. 2008;222(8):959-968.
16. Rankouhi B, Javadpour S, Delfanian F, Letcher T. Failure Analysis and Mechanical Characterization of 3D Printed ABS With Respect to Layer Thickness and Orientation. J Fail Anal Prev. 2016;16(3):467-481.
17. Boschetto, Giordano, Veniali. 3D roughness profile model in fused deposition modelling. Rapid Prototyp J. 2013;19(4):240-252.
18. Fodran E, Koch M, Menon U. Mechanical and dimensional characteristics of fused deposition modeling build styles. In: Solid Freeform Fabrication Proceedings. Austin, TX: University of Texas at Austin; 1996:419-442.
19. Rodríguez JF, Thomas JP, Renaud JE. Mechanical behavior of acrylonitrile butadiene styrene (ABS) fused deposition materials. Experimental investigation. Rapid Prototyp J. 2001;7(3):148-158.

Preprint version. Final publication in 3D PRINTING AND ADDITIVE MANUFACTURING Volume 3, Number 3, 2016. It is available from Mary Ann Liebert, Inc., publishers http://dx.doi.org/10.1089/3dp.2015.0036

20. Rodríguez JF, Thomas JP, Renaud JE. Mechanical behavior of acrylonitrile butadiene styrene fused deposition materials modeling. Rapid Prototyp J. 2003;9(4):219-230.
21. Gurrala PK, Regalla SP. Part strength evolution with bonding between filaments in fused deposition modelling. Virtual Phys Prototyp. 2014;9(3):141-149.
22. Montero M, Roundy S, Odell D, Ahn S-H, Wright PK. Material characterization of fused deposition modeling (FDM) ABS by designed experiments. In: Proceedings of Rapid Prototyping and Manufacturing Conference, SME. Cincinnati, Ohio; 2001:1-21.
23. Ziemian CW, Sharma MM, Ziemian SN. Anisotropic Mechanical Properties of ABS Parts Fabricated by Fused Deposition Modelling. In: Gokcek M, ed. Mechanical Engineering. New York, NY, USA: InTech; 2012:159-180.
24. Croccolo D, De Agostinis M, Olmi G. Experimental characterization and analytical modelling of the mechanical behaviour of fused deposition processed parts made of ABS-M30. Comput Mater Sci. 2013;79:506-518.
25. Baich L, Manogharan G. Study of infill print parameters on mechanical strength and production cost-time of 3d printed abs parts. In: International Solid Freeform Fabrication Symposium. Austin, TX; 2015:209-2018.
26. Lanzotti A, Grasso M, Staiano G, Martorelli M. The impact of process parameters on mechanical properties of parts fabricated in PLA with an open-source 3-D printer. Rapid Prototyp J. 2015;21(5):604-617.
27. Akande SO, Dalgarno KW, Munguia J. Low-Cost QA Benchmark for Fused Filament Fabrication. 3D Print Addit Manuf. 2015;2(2):78-84.
28. Qureshi AJ, Mahmood S, Wong WLE, Talamona D. Design for Scalability and Strength Optimisation for components created through FDM process. In: Weber C, Husung S, eds. Proceedings of the 20th International Conference on Engineering Design (ICED 15) Volume 6: Design Methods and Tools - Part 2. ; 2015:255-266.
29. Lanzotti A, Martorelli M, Staiano G. Understanding Process Parameter Effects of RepRap Open-Source Three-Dimensional Printers Through a Design of Experiments Approach. J Manuf Sci Eng. 2015;137(1):11017.
30. Afrose MF, Masood SH, Iovenitti P, Nikzad M, Sbarski I. Effects of part build orientations on fatigue behaviour of FDM-processed PLA material. Prog Addit Manuf. 2016;1(1):21-28.
31. 3DHubs.com. 3D Printing Trends June 2016. https://www.3dhubs.com/trends. Published 2016. Accessed January 1, 2015.
32. Ranellucci A. Reprap, Slic3r and the Future of 3D Printing. In: Canessa E, Fonda C, Zennaro M, eds. Low-Cost 3D Printing for Science, Education & Sustainable Development. Trieste, Italy: ICTP; 2013:75-82.
33. Hodgson G, Ranellucci A, Moe J. Slic3r Manual - Infill Patterns and Density. http://manual.slic3r.org/expert-mode/infill. Published May 2014. Accessed May 15, 2016.
34. 3mm ABS Filament Nature - Torwell. http://www.torwell3d.com. Accessed June 6, 2016.
35. Riddick JC, Haile MA, Wahlde R Von, Cole DP, Bamiduro O, Johnson TE. Fractographic analysis of tensile failure of acrylonitrile-butadiene-styrene fabricated by fused deposition modeling. Addit Manuf. 2016;11:49-59.
36. Roxas M. Fluid dynamics analysis of desktop-based fused deposition modeling rapid prototyping. 2008.
37. Wittbrodt B, Pearce JM. The Effects of PLA Color on Material Properties of 3-D Printed Components. Addit Manuf. 2015;8:110-116.

Address correspondence to:
Miguel Fernandez-Vicente
Instituto de Diseño y Fabricación
Universitat Politècnica de València
Camino de Vera s/n
46022 Valencia
Spain

E-mail: mifervi@upv.es

Preprint version. Final publication in 3D PRINTING AND ADDITIVE MANUFACTURING Volume 3, Number 3, 2016. It is available from Mary Ann Liebert, Inc., publishers http://dx.doi.org/10.1089/3dp.2015.0036